

## Case I Coherence Effects

### Ultrasonic Attenuation

$$H_{pert} = \lambda q u_0 e^{i(qx - \omega t)} \sum_{k, k', \sigma, \sigma'} C_{k\sigma}^+ C_{k'\sigma'}$$

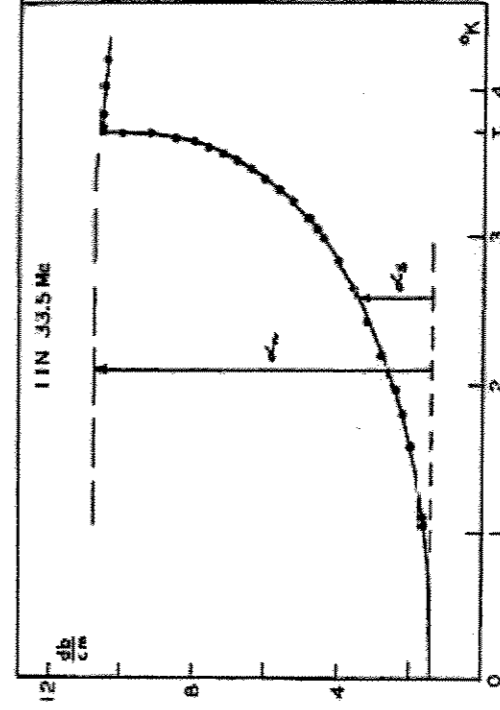


FIG. 1. Measured ultrasonic attenuation of longitudinal waves in a tin single crystal at a frequency of 33.5 Mc/sec.

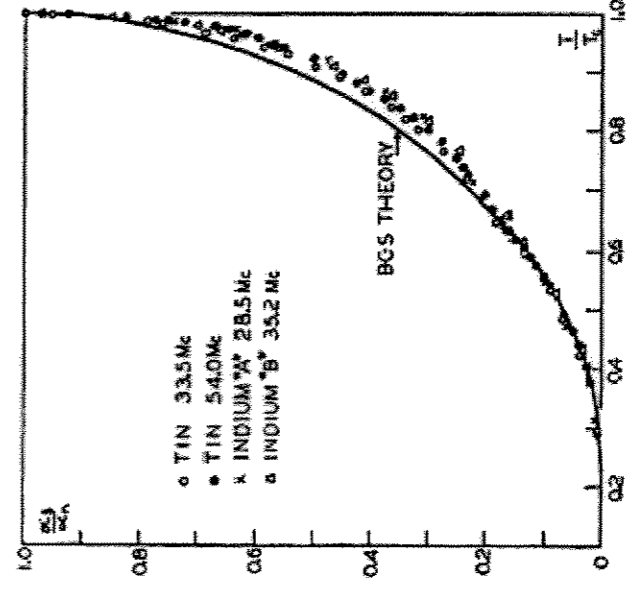


FIG. 2. Measured values of  $\alpha_c/\alpha_0$  compared with the theoretical variation of Bardeen, Cooper, and Schrieffer assuming  $\epsilon_0(0) = 1.75kT_c$ . For tin  $T_c^0 = 3.71$  °K and for indium  $T_c^0 = 3.40$  °K.

R. W. Morse and H. V. Bohm, Phys. Rev. **108**, 1094 (1957)

L. C. Hebel and C. P. Slichter, *Phys. Rev.* **113**, 1504 (1959).

### Hebel-Slichter Coherence Peak

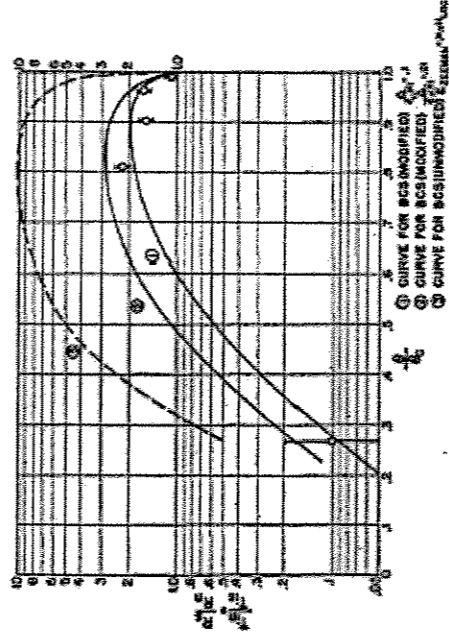


FIG. 3. Relaxation rate in a superconductor,  $K_1$ , relative to the zero-field value extrapolated from the normal state,  $K_1(0)$ , versus reduced temperature  $\theta/b_0$ . The three theoretical curves within BCS theory are described in the text.

### Case II Coherence Effects

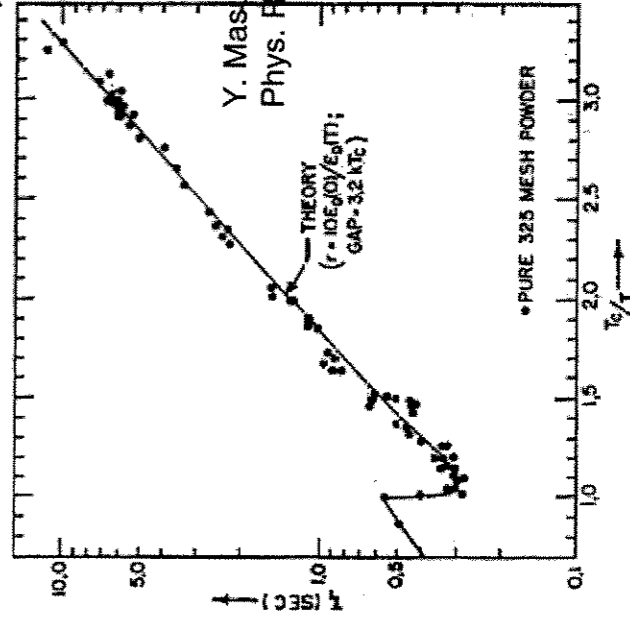


FIG. 2. Measured values of  $T_1$  in the powdered sample. No points were rejected, so that the scatter gives a fairly good idea of the accuracy.  $T_0$  was taken to be 1.178°K. The theoretical curve is the same as the solid line of Fig. 5.

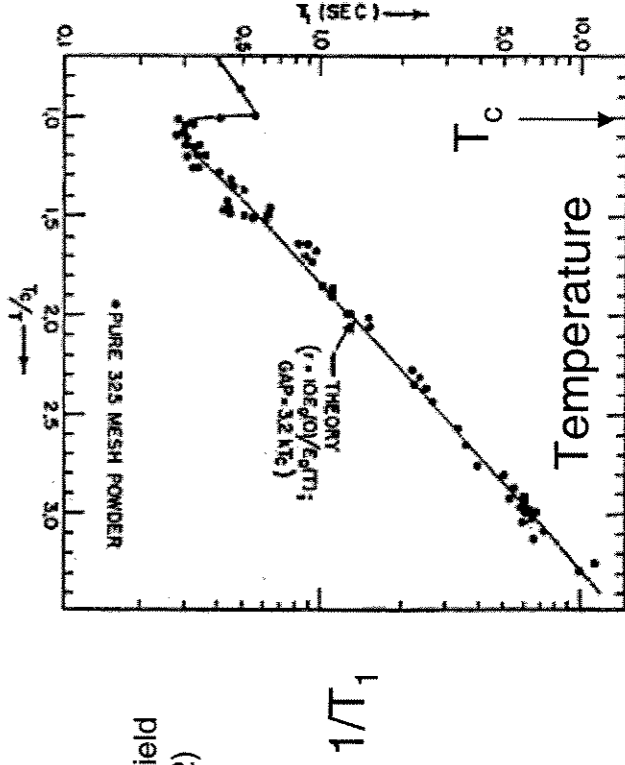
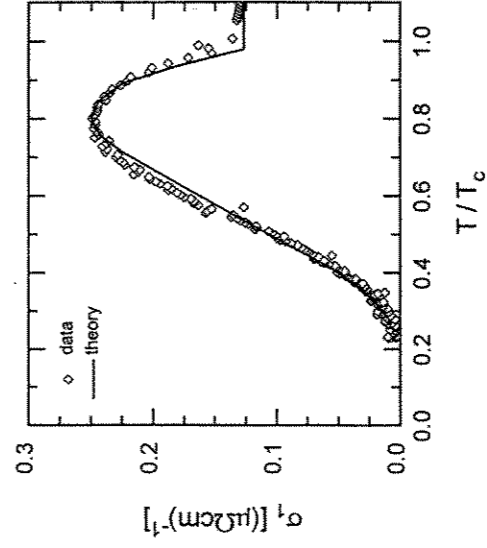


FIG. 2. Measured values of  $T_1$  in the powdered sample. No points were rejected, so that the scatter gives a fairly good idea of the accuracy.  $T_0$  was taken to be 1.178°K. The theoretical curve is the same as the solid line of Fig. 5.

## Case II Coherence Effects in $\sigma_1(T)$

Nb<sub>3</sub>Sn



**"BCS Coherence Peak"**

Fig. 2.12. Temperature dependent quasi-particle conductivity  $\sigma_1(T)/\sigma_1(T_c)$ , deduced from the data at 87 GHz in Fig. 2.10 after subtraction of the residual surface resistance, compared with the expectation from BCS theory for low frequencies [98] (see Fig. 1.7 in Sect. 1.3.2).

Nb<sub>3</sub>Sn and Cuprate

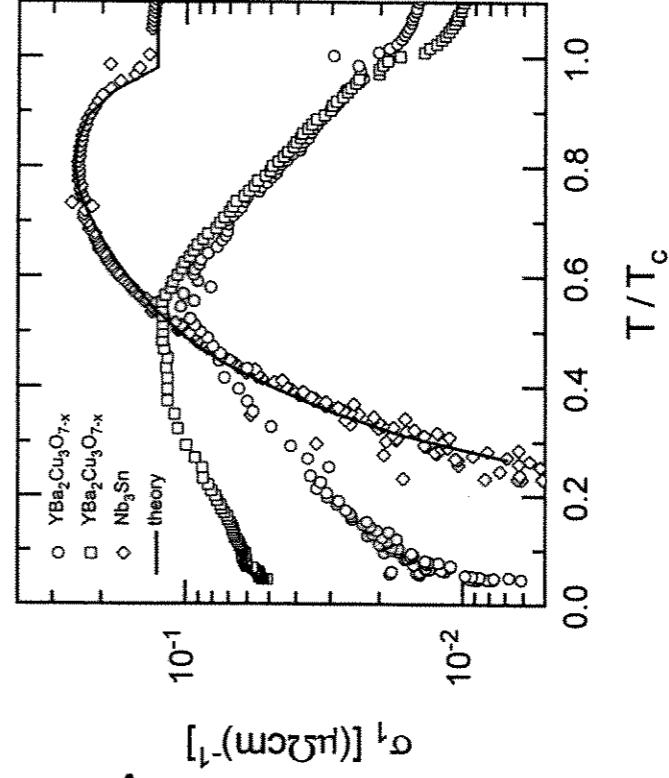


Fig. 2.20. Quasi-particle conductivity  $\sigma_1(T)$  versus  $T/T_c$  for two epitaxial YBCO films (circles and squares), and a Nb<sub>3</sub>Sn film on sapphire prepared by TVD (Fig. 2.12). Also shown is the low-frequency expectation for the coherence peak at 2% smearing of the energy gap (solid line, see Fig. 1.7).

as described in the following letter.  
 dashed curve is one proposed for the data. The  
 points on these curves are determined by the  
 power width of the composite spectrum used.  
 The frequency uncertainty is indicated by the  
 error bars. The normal transmission ratio of  
 the normal state is  $T_{11} = 0.0001$  (see text).  
 The normal transmission ratio of the normal  
 state is  $T_{11} = 0.0001$  (see text).  
 The normal transmission ratio of the normal  
 state is  $T_{11} = 0.0001$  (see text).

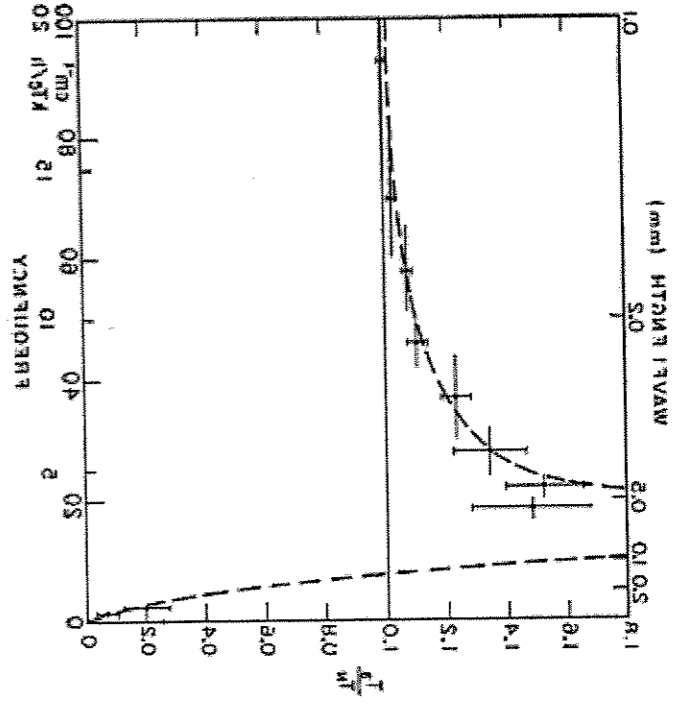


Fig. 1. Experimental transmission ratio of superconducting junction.

where  $n$  is the refractive index of the substrate.  
 according to the calculation of Mattis and Bickers. The transmission curve is for a thin resistor  $R \ll \hbar v_F$  (see text).  
 The frequency dependence of  $\sigma_{xx}$  and  $\sigma_{yy}$  is shown in Fig. 10.

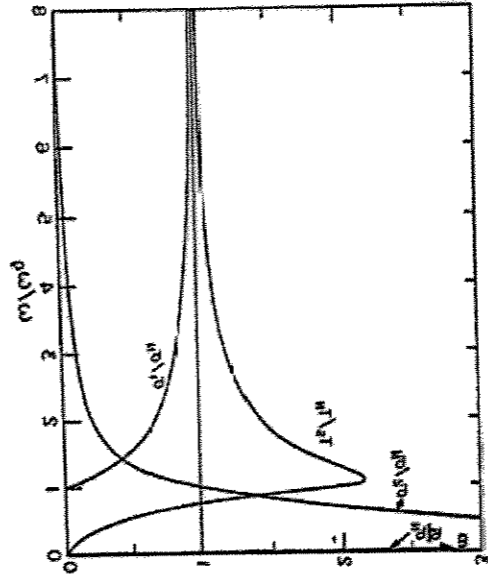


Fig. 10. Frequency dependence of  $\sigma_{xx}$  and  $\sigma_{yy}$  for a thin resistor  $R \ll \hbar v_F$  (see text). The solid curve is calculated using the measured film resistance, the dashed curve is calculated using the dependence of  $\sigma_{xx}$  for  $T=0$ . The solid curve is the calculated value. (See text.)

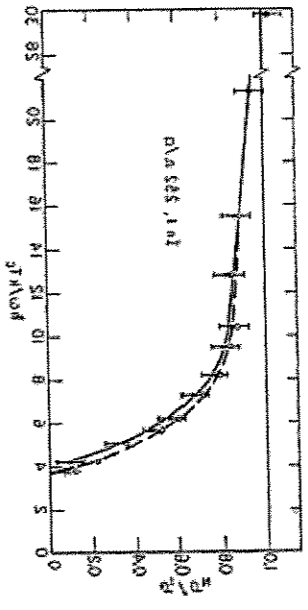


Fig. 8. Frequency dependence of  $\sigma_{xx}$  for a thin resistor  $R \ll \hbar v_F$  (see text). The solid curve is calculated using the measured film resistance, the dashed curve is calculated using the dependence of  $\sigma_{xx}$  for  $T=0$ . The solid curve is the calculated value. (See text.)

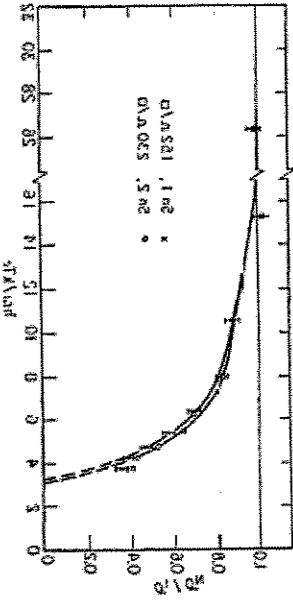


Fig. 9. Frequency dependence of  $\sigma_{yy}$  for a thin resistor  $R \ll \hbar v_F$  (see text). The solid curve is calculated using the measured film resistance, the dashed curve is calculated using the dependence of  $\sigma_{yy}$  for  $T=0$ . The solid curve is the calculated value. (See text.)

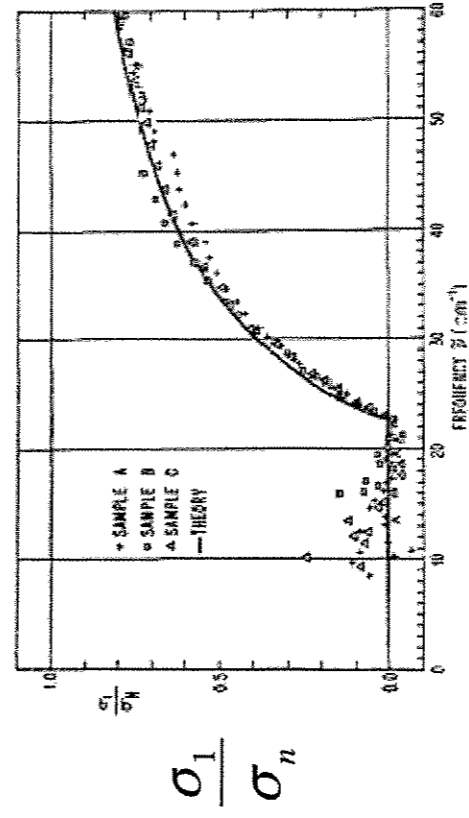


FIG. 3. Results of measurements of the real part of the normalized conductivity of three thin lead films at 2°K, compared with Mottis-Barddeen theory with gap frequency fitted to 22.5 cm<sup>-1</sup>. To reduce the clutter in the figure, only about one fourth as many points are shown as were taken and recorded in Ref. 7. The points shown are selected typical points above the gap and local averages below the gap.

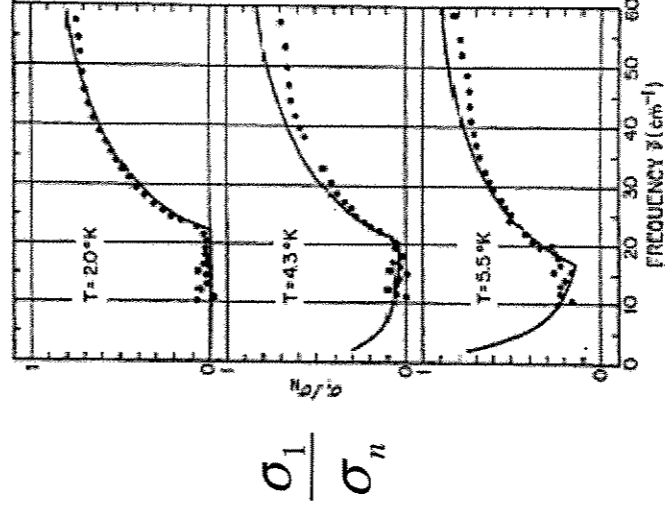


FIG. 4. Temperature and frequency dependence of normalized conductivity  $\sigma_1/\sigma_n$  in a thin superconducting lead film (sample C), compared with predictions of Mottis-Barddeen theory (calculated with the assistance of a program supplied by Harris), shown as solid curve. The gap frequency was fitted only for the low-temperature limit. The number of data points shown has been reduced as in Fig. 3.